Osteoblast attachment and mineralized nodule formation on rough and smooth 45S5 bioactive glass monoliths

J.E. Gough, I. Notingher, L.L. Hench
Department of Materials, Imperial College, Prince Consort Rd, London, SW7 2BP, UK

Received 3 June 2003; revised 7 August 2003; accepted 27 August 2003

Abstract: Human primary osteoblast responses to smooth and roughened bioactive glass of 45S5 (Bioglass™) composition (46.1% SiO_2, 26.9% CaO, 2.6% P_2O_5, 24.4% Na_2O) were analysed *in vitro.* The smooth and rough surfaces had R_a values and peak to valley distances of 0.04, 4.397, 2.027, and 21.328 μm, respectively. Cell attachment and morphology was observed using phalloidin staining of the actin cytoskeleton and revealed significant differences between smooth and rough surfaces. Cells that were spiky in appearance on the rough compared to the smooth surface formed an organized actin matrix much later on the rough surface. Scanning electron microscopy revealed many cell filipodia extending from more rounded cell bodies on the rough surface. A significantly greater number of nodules on the rough surface was observed, and these were shown to mineralize when supplemented with beta-glycerophosphate and dexamethasone. Raman spectroscopy confirmed the presence of hydroxyapatite in the mineralized cultures showing a definite peak at 964 cm^{-1}. FTIR analysis showed hydroxyapatite formation occurred more rapidly on the rough surface. This study demonstrates that although initial cell morphology was less advanced on the roughened surface, the cells were able to form mineralized nodules in greater numbers. This may have implications to bone tissue engineering using bioactive glasses. © 2004 Wiley Periodicals, Inc. J Biomed Mater Res 68A: 640–650, 2004

Key words: bioactive glass; osteoblast; mineralization; hydroxyapatite; topography

INTRODUCTION

Bioactive glasses were first reported by Hench et al.[1] in 1971, and were originally composed of oxides of calcium, phosphate, silica, and sodium. Due to their ability to bond to living bone, [2] various bioactive glasses and ceramics have undergone extensive research in the field of bone repair and bone tissue engineering.[3–5] Bioactive glasses rapidly form a hydroxyapatite layer on the surface in simulated body fluids, which lends to their bone-bonding ability.[1,6,7]

Topography is known to influence cell responses.[8] A wide variety of cells are able to detect changes in the surface topography, and much research has been aimed at grooves and ridges of varying dimensions.[9,10] Producing materials with grooved, and roughened surfaces has therefore undergone extensive research to try to control cell behavior on potential implant materials. Osteoblasts have been investigated on a variety of roughened surfaces.[11–13]

Raman spectroscopy is a well-established technique for studying biological samples and living cells in cultures.[14–16] It has also been used to detect mineralisation of mouse calvaria cells.[17]

This study investigates human osteoblast attachment and nodule formation on Bioglass™ monoliths with a smooth or roughened surface. Mineralization of nodules was analyzed using alizarin red staining and also Raman spectroscopy of live osteoblast cultures.

METHODS

45S5 Bioglass monoliths measuring 15 mm diameter × 2 mm depth, with one side bearing a 3-μm finish, were generously provided by David Greenspan, US Biomaterials. Monoliths were preincubated in culture medium for 24 h prior to cell seeding.

Surface topography

The surface topographical features of the monoliths were analyzed by optical interferometry using a NewView200

Correspondence to: J.E. Gough, Manchester Materials Science Centre, UMIST and The University of Manchester, Grosvenor Street, Manchester, M1 7HS,
Contract grant sponsor: MRC

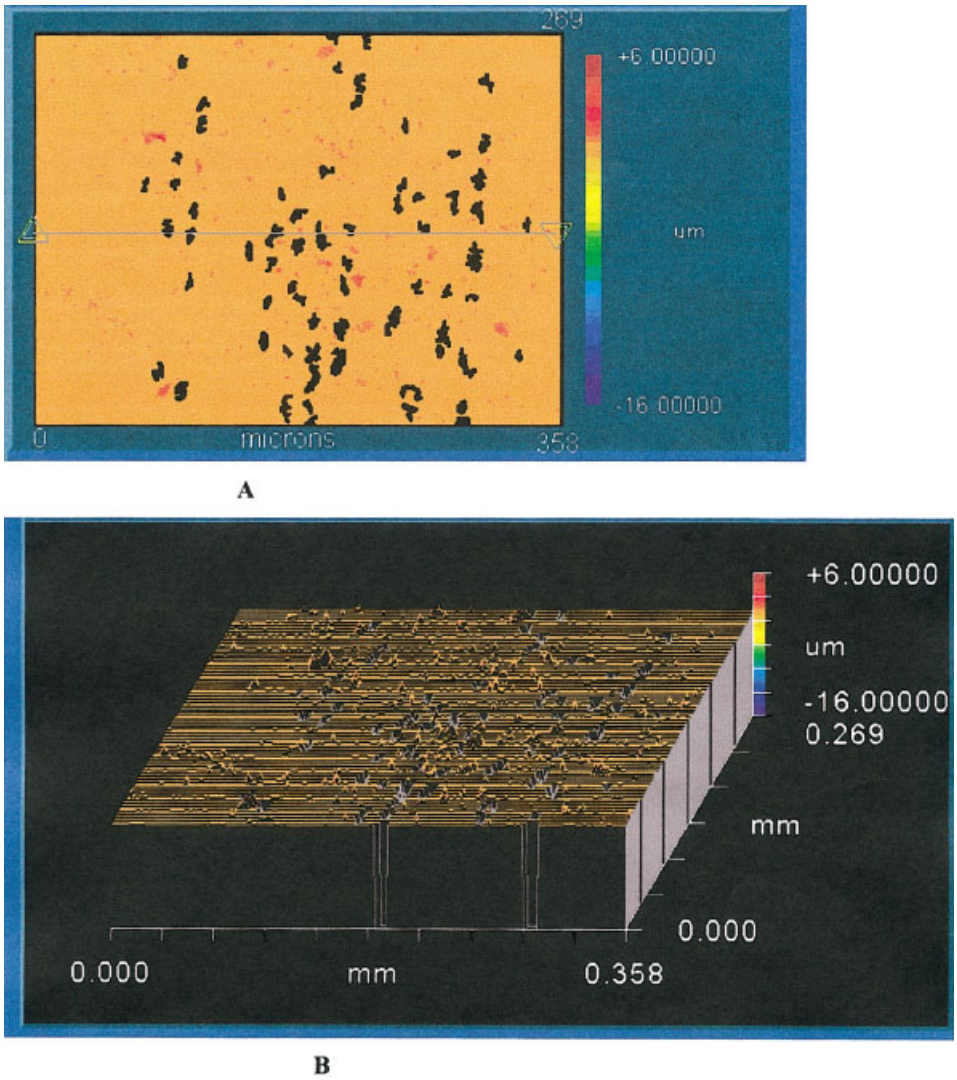

Figure 1. Zygo 3D surface analysis of the smooth 45S5 sample. (A) 2D profile, (B) 3D profile. Peak to valley distance (PV) was found to be 4.397 μm and R_a value was 0.045 μm. [Color figure can be viewed in the online issue, which is available at www.interscience.wiley.com.]

microscope (Zygo Corporation). A 10× objective and 2× zoom were used for a lateral resolution of 1.12 μm. Various positions on the samples were measured to ensure that the images were representative of the whole surface.

Osteoblast culture

Human primary osteoblasts (HOBs) were isolated as described previously from excised femoral heads after total hip replacement surgery.[18,19] Trabecular bone was cut into fragments of approximately 3 × 3 mm and washed several times in phosphate buffered saline (PBS) to remove blood cells and debris, with a final wash in culture medium.

Fragments were then cultured in complete Dulbecco's Modified Eagles Medium (DMEM) containing 10% foetal bovine serum (FBS) with 2% penicillin/streptomycin and 0.85 m*M* ascorbic acid. The fragments were incubated at 37°C in a humidified incubator with 5% CO_2. After culture for 7–10 days, fragments were subjected to trypsin (0.02%) and collagenase (0.162 U/mL) digestion for 20 min at 37°C on a roller mixer. The resulting cell suspension was then centrifuged at 1000 rpm and enzyme digestion of the fragments repeated. This process was performed a total of five times and cells pooled. HOBs were cultured as described above on Bioglass samples or on tissue culture plastic or Thermanox™ discs as positive controls, at a density of 80,000 cells/cm^2.

Actin cytoskeleton staining

Cells were cultured for 15, 30, 60, and 90 min, 4 and 48 h on Bioglass or Thermanox™ controls. Samples were washed in PBS and fixed with 4% paraformaldehyde for 10 min at room temperature. Samples were washed again and permeabilized for 5 min at −20°C. Cells were then washed in 1% bovine serum albumin (BSA) in PBS and stained with 10

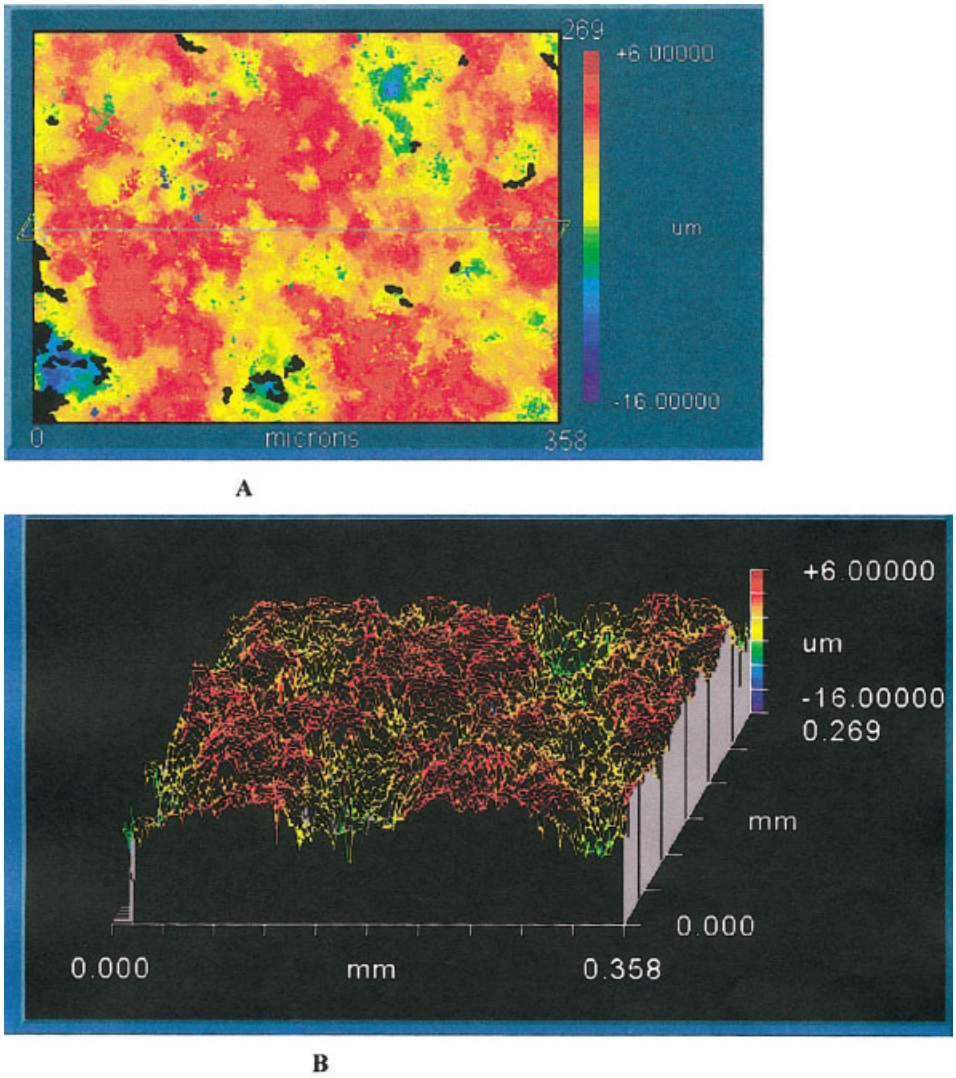

Figure 2. Zygo 3D surface analysis of the rough 45S5 sample. (A) 2D profile, (B) 3D profile. Peak to valley distance (PV) was found to be 21.328 μm and R_a value was 2.027 μm. [Color figure can be viewed in the online issue, which is available at www.interscience.wiley.com.]

μg/mL FITC-conjugated phalloidin (Molecular Probes, Engene, OR) for 20 min at room temperature. Samples were washed in BSA/PBS and counterstained with 5 μg/mL propidium iodide in PBS. Samples were washed again and mounted under glass coverslips with Vectashield and viewed using a BioRad confocal microscope.

Determination of degree of spreading and actin organization

After actin staining as above, cells were viewed using a confocal microscope at ×200 and ×400 original magnification and scored according to the Sinha method.[20] Cells displaying faint staining with no discernible actin filament organization were labeled "Type I," cells displaying cortical filaments below the cell membrane with some radially oriented filaments were termed "Type II," and cells displaying distinct well-formed actin filaments parallel to one another and the long axis of the cell were termed "Type III." For each sample (prepared in triplicate) five fields of view were observed and counted to quantify level of spreading and actin organization.

Scanning electron microscopy

Cells were cultured on Bioglass™ and Thermanox™ discs for 90 min and fixed in 1.5% glutaraldehyde for 30 min at 4°C. Cells were then postfixed in 1% osmium tetroxide for 1 h at 4°C. Cells were dehydrated through a series of increasing concentrations of ethanol and dried using hexamethyldisilazane (HMDS). Samples were sputter coated with gold and viewed using a Cambridge Stereoscan S360 scanning electron microscope operated at 10 kV.

Nodule formation

The number of nodules formed on the surfaces was assessed by light microscopy. Samples were viewed at 5 days

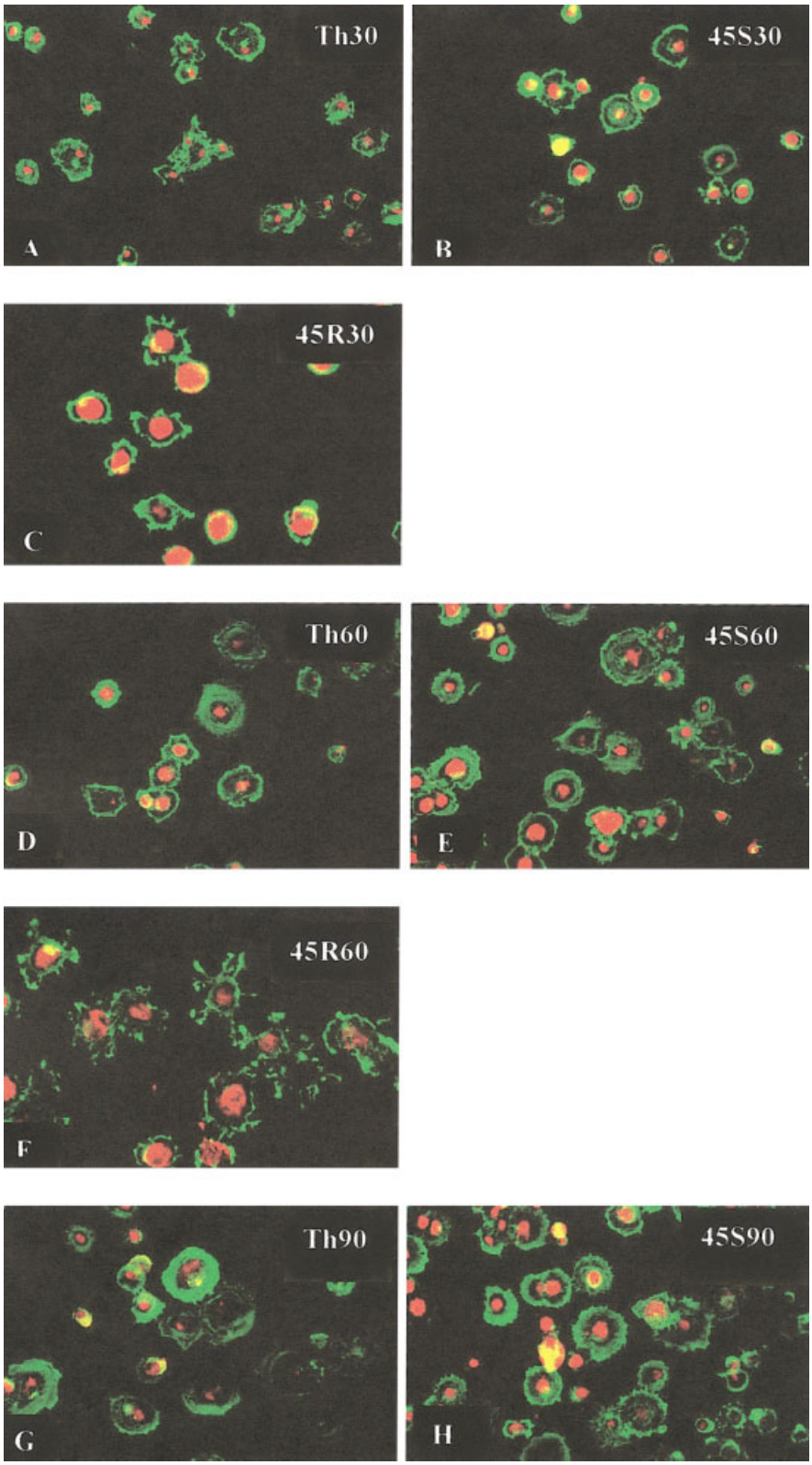

Figure 3. Confocal fluorescence micrographs showing actin staining of osteoblasts cultured on Thermanox™ control (A, D, G, J, M), smooth (45S) (B, E, H, K, N) and rough (45R) (C, F, I, L, O) Bioglass for 30 (A, B, C), 60 (D, E, F), 90 (G, H, I) minutes, 4 (J, K, L) and 48 h (M, N, O). Originial magnification ×200 (except J, which is ×400). [Color figure can be viewed in the online issue, which is available at www.interscience.wiley.com.]

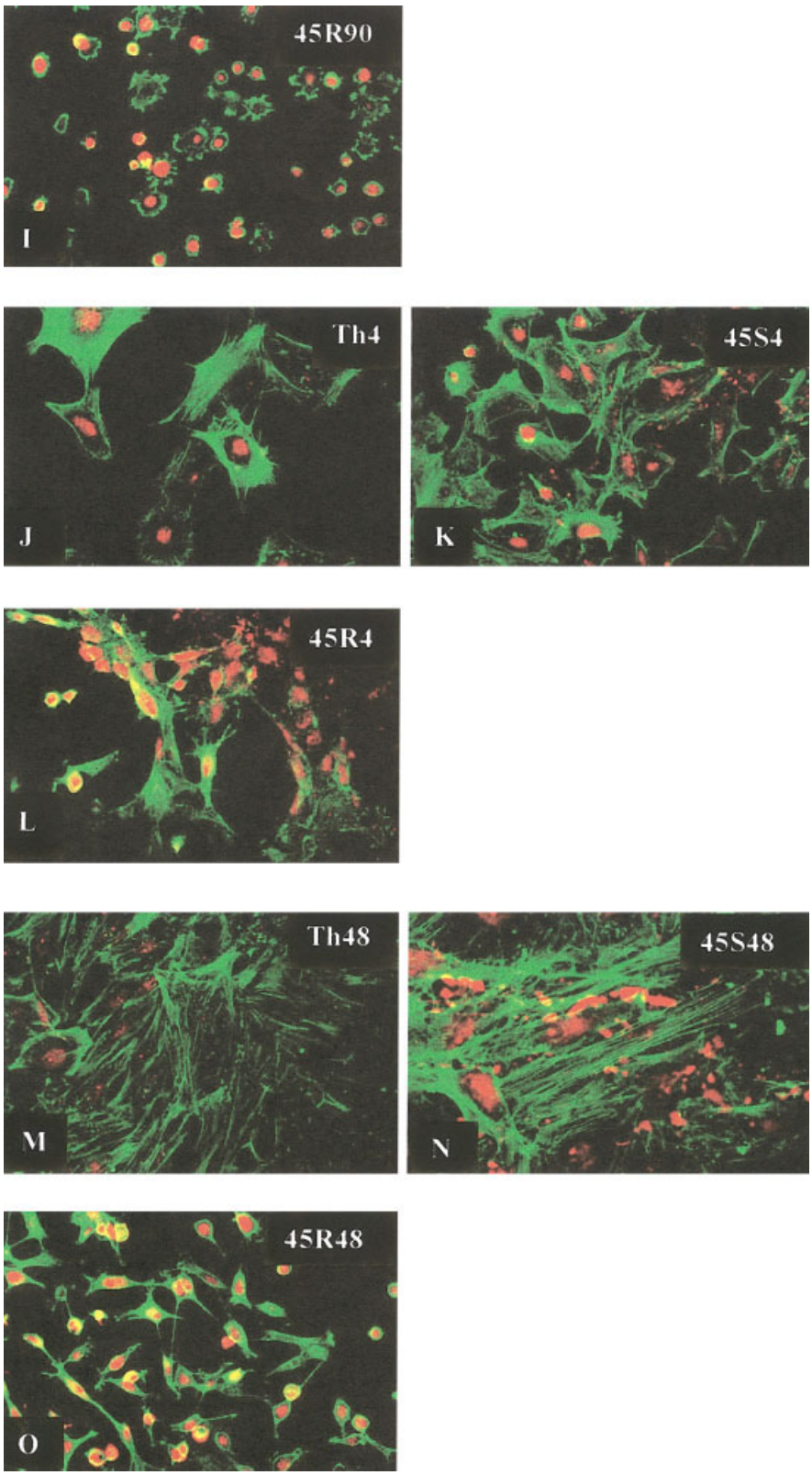

Figure 3 (*Continued from the previous page*)

and 14 days using a light microscope, and the number of nodules formed in each well counted.

Mineralization—alizarin red and raman spectroscopy

Cells were cultured with or without 10 m*M* beta-glycerophosphate (BGP) and 100 n*M* dexamethasone (Dex) (Sigma, Dorset UK). Staining of calcium deposits was performed using Alizarin Red S (Sigma, Dorset, UK). Cells were cultured for time points up to 28 days then rinsed in PBS and fixed in 70% ice cold ethanol, rinsed in distilled water, and stained for 2 min in 1% Alizarin Red S solution. Cells were then rinsed in distilled water several times and mounted under glass cover slips using PBS/glycerol.

Confirmation of the presence of hydroxyapatite was performed using Raman spectroscopy. Raman spectra were measured with a Renishaw 2000 spectrometer connected to a Leica microscope. The microscope was equipped with a long working distance (2 mm) water immersion objective, magnification 63×, NA 0.9. A high-power near-infrared laser was used for excitation: 100 mW at 785 nm. At this wavelength, long time periods of irradiation can be carried out without damaging the cells.[14] The spectra were collected over 40 s. During the Raman experiments the cultures were kept in PBS.

Hydroxyapatite formation on bioglass™ surface

Fourier transform infrared spectroscopic (Genesis II FTIR, Spectronic Unicam) analysis was conducted using KBr pellets (1:100 weight ratio). Scans were taken between 1600–400 cm^{-1}.

RESULTS

Surface topographical features of the smooth and rough surfaces differed as shown in Figures 1 (smooth) and 2 (rough). Peak to valley distance of the smooth sample measured 4.397 μm compared to 21.328 μm for the rough surface. The Ra values measured 0.045 μm for the smooth surface and 2.027 μm for the rough surface.

Cell attachment and spreading was evaluated using actin cytoskeletal staining (Fig. 3) and cell scoring (Fig. 4).

A marked difference in degree of spreading was observed when comparing Thermanox™ control (Th), smooth Bioglass (45S), and roughened Bioglass (45R). After 30 min of attachment, cells on the Th [Fig. 1(A)] and 45S [3(B)] surfaces were similar in morphology and actin organization, whereas cells on the 45R [3(C)] surface appeared "spiky" in morphology, with prominent actin staining in projections from the main cell body. These observations were more evident after 60

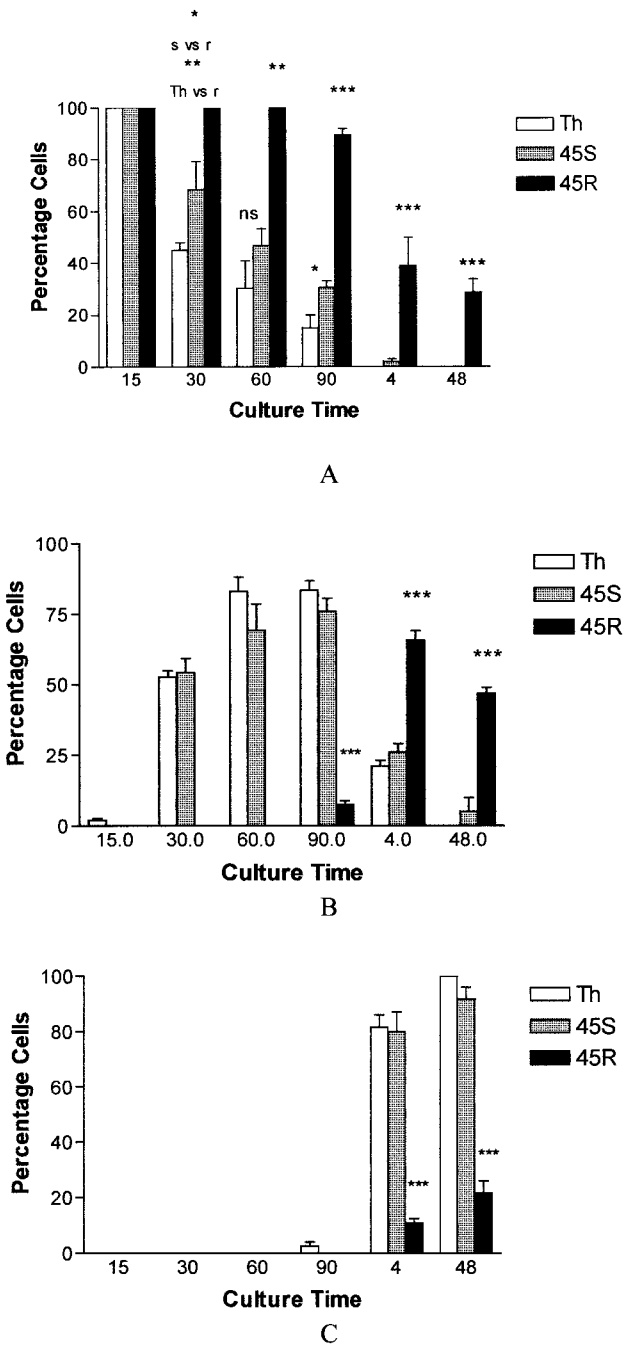

Figure 4. Graph showing percentages of Type I cells (A), Type II cells (B) and Type III cells (C), i.e., level of actin organization, after culture for 15 min to 48 h. Analysis of variance with Tukey–Kramer posttest was carried out on samples where $n = 3 \pm$ standard error of the mean. Values are denoted significantly different where $p = < 0.05$ (*), $p = <0.001$ (**) and $p = <0.0001$ (***).

[Fig. 3(D), (E), (F)] and 90 min culture [Fig. 3(G), (H) and (I)]. After 4 h in culture, again the Th [Fig. 3(J)] and 45S [Fig. 3(K)] were similar in morphology with a well-organized actin cytoskeleton demonstrating Type II and Type III cells. Cells on the 45R sample [Fig. 3(L)], however, showed few radially or parallel

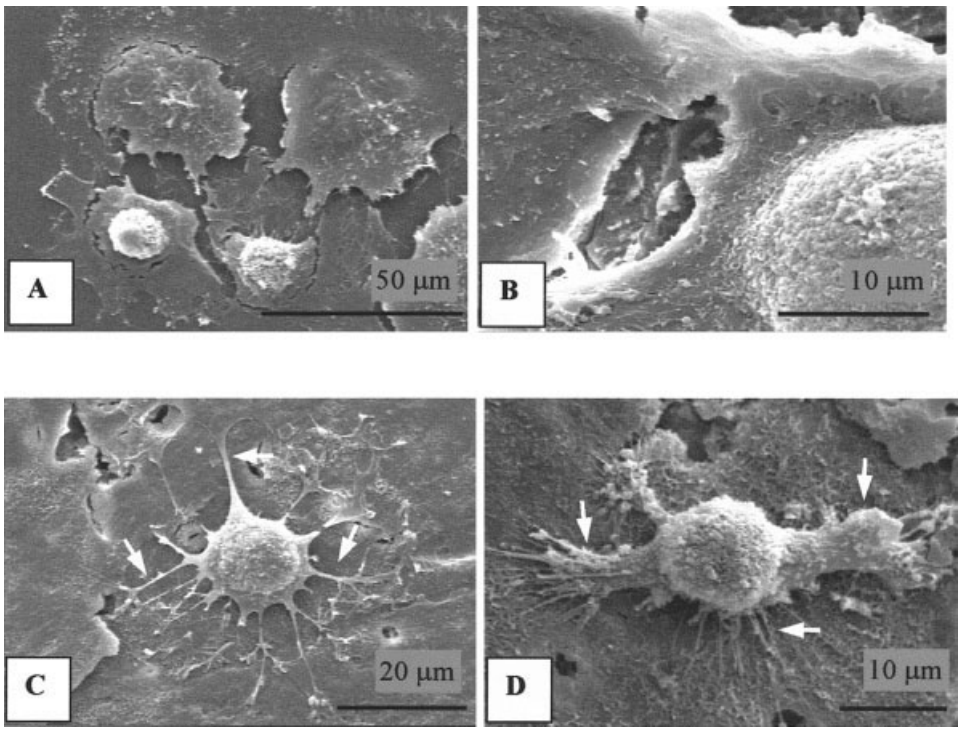

Figure 5. Scanning electron micrographs of HOBs cultured on Thermanox™ (A) × 750, 45S (B) × 3400, and 45R (C, × 1400 and D, × 2800) for 90 mins. Arrows highlight filopodia on the 45R surfaces.

orientated actin fibers, instead the fibers were orientated along the long axis of the cell and at the cell periphery. By 48 h cells on the Th [Fig. 3(M)] and 45S [Fig 3(N)] were fully spread demonstrating Type III morphology with all cells showing parallel actin fiber arrangement. Cells on the 45R sample [Fig. 3(O)] were very different in appearance with many cells still bearing a Type I and II morphology. Quantification of actin organization is shown in Figure 4. Percentage of Type I cells is shown in 4(A), Type II cells in 4(B), and Type 3 cells in 4(C). Cells cultured on Thermanox™ control and 45S surface had similar actin organization throughout the time points studied, with cells changing rapidly from Type I through to Types II and III. On the 45R surface, however, the majority of cells remained in the Type II conformation, even after 48 h of culture.

The spiky morphology of cells cultured on the 45R surface was also evident when analyzed by scanning electron microscopy (Fig. 5). Cells cultured on Thermanox™ (A) and 45S (B) showed a smooth, flattened morphology compared to the spiky and more three-dimensional main cell body as shown in (C) and (D).

Nodule formation was observed on both 45S and 45R, but no nodules were seen in the time period covered on Th samples. Quantification of numbers of nodules formed is shown in Figure 6, where it can be seen that a significantly higher number of nodules were seen on the 45R sample at 5 and 14 days.

These nodules were then analysed for mineralization using alizarin red staining of calcium deposits, as shown in Figure 7, where a positively stained nodule can be seen. Raman spectroscopy was then used to confirm hydroxyapatite formation within the nodules as shown in Figures 8 and 9. Raman spectra of osteoblasts on smooth and rough Bioglass™ discs without being fed with BGP and Dex are shown in Figure 8.

The Raman spectra contain contribution from all components of cells: proteins, nucleic acids, lipids, and carbohydrates.[16] The peak assignment is given in Table I.[16]

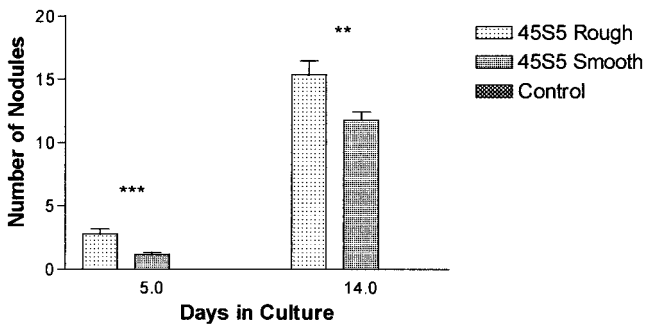

Figure 6. Graph showing number of nodules formed on Thermanox™ control, smooth and rough Bioglass after 5 and 14 days in culture. Analysis of variance with Tukey–Kramer posttest was carried out on samples where $n = 3 \pm$ standard error of the mean. Values are denoted significantly different where $p = <0.001$ (**) and $p = <0.0001$ (***). No nodules formed on the tissue culture plastic control over the time period studied.

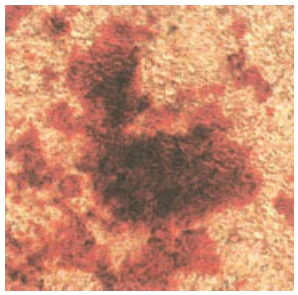

Figure 7. Light micrograph of alizarin red staining of nodules after culture on 45S5 and supplementation with beta-glycerophosphate and dexamethasone for 12 days. [Color figure can be viewed in the online issue, which is available at www.interscience.wiley.com.]

Figure 9 shows the Raman spectra of bone nodules formed on rough and smooth Bioglass from cells supplemented with BGP and Dex. In this case, a stronger peak is present at 964 cm^{-1} (compared to that in Fig. 8), which corresponds to the symmetric stretching vibration of P–O in PO_4^{3-} tetrahedra of hydroxy apatite crystals.[21] The magnitude of this peak is much stronger than the peaks corresponding to organic molecules in cells. This peak indicates a high degree of mineralization of the bone nodule when the osteoblast medium was supplemented with BGP and Dex.

Hydroxyapatite formation was observed on both rough and smooth surfaces after 24-h incubation in culture medium using FTIR. As shown in Figure 10(a) and 10(b), the rough surface showed prominent HA formation (594, 584, 571 cm^{-1}), whereas very little HA formation was observed on the smooth surface, as shown in Figure 11, in the time period tested.

DISCUSSION

Cell attachment and spreading is known to affect the long-term phenotype of anchorage dependent

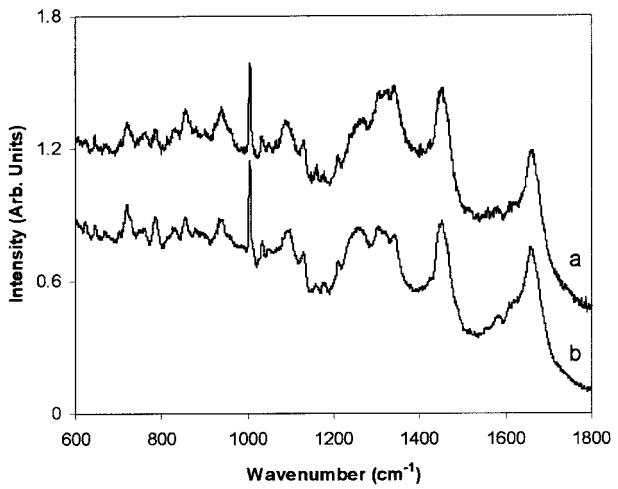

Figure 8. Raman spectra of osteoblasts on Bioglass without BGP and Dex: (a) smooth surface, (b) rough surface.

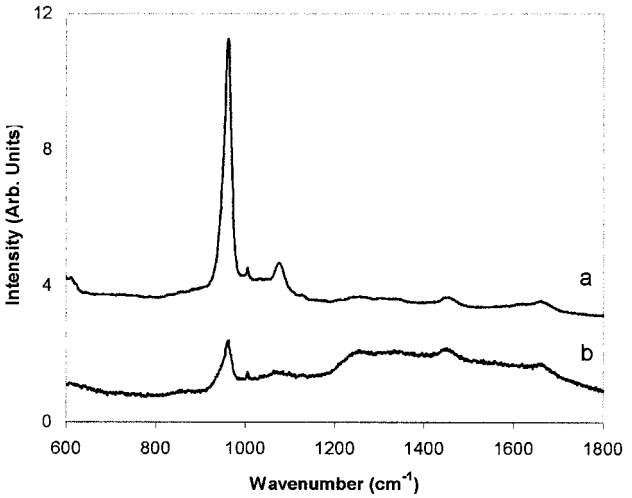

Figure 9. Raman spectra of osteoblasts on BG fed with BGP: (a) smooth surface, (b) rough surface.

cells,[12] where highly organized and orientated extracellular matrix was observed on smooth surfaces compared to rough surfaces. Cell morphology as shown by scanning electron microscopy and cytoskeletal staining differs depending on the substrate to which the cells are attached.[12] Osteoblasts, for example, are well documented in the literature, and it can be seen that on some surfaces they appear extremely flattened and on other surfaces they have a more three-dimensional morphology.[22] The topography of a surface can profoundly effect cell attachment and spreading, and it is generally thought that a roughened surface is preferential to strong bone bonding at the tissue–implant interface.[11,23]

In this study we examined osteoblast responses to a smooth 45S5 monolith and a roughened 45S5 monolith. Significant differences in cell morphology were observed using scanning electron microscopy and confocal and fluorescence microscopy of actin staining. Cells appeared more spread and more flattened against the substrate surface on the 45S compared to the 45R. Cells on the 45R surface, in fact, did not reach what is thought to be the ideal level of actin organization, i.e., a "Type III" conformation even after 48 h of culture. The study then went on to determine what effect these differences have on nodule formation and mineralization. The number of nodules formed on the two surfaces was also significantly different, with a greater number of nodules being formed on the roughened surface (45R). Why this is so, we cannot yet explain, however, the less flattened and spread morphology or a more three-dimensional morphology may promote faster nodule formation and a higher number of nodules formed.

Cells that have a more "spiky" or stellate appearance have been observed in the literature when cultured on roughened surfaces.[12] It is known that filop-

TABLE I
Peak Assignment for Raman Spectra (A, G, C, T-Adenine, Guanine, Cytosine, Thymine; str., tw., br.-Stretch, Twist, Breadth)[3]

Peak Position (cm^{-1})	Assignment			
	DNA/RNA	Proteins	Lipids	Carbohydr
1659		Amide I α-helix	C=C str.	
1449		CH def	CH def	CH def
1300			=CH def	
↓		Amide III	=CH def	
1230				
1095	PO_2^- str.		Chain C—C str.	C—C str
1005		Ring br Phe		
937		C—C BK str. α-helix		
788	O—P—O str.		O—P—O	
782	U,C,T ring br			
729	A			
669	T, G			
645		C—C tw Tyr		
623		C—C tw Phe		

odia or microspikes of cells are used in sensing the substrate. Microspikes of neurons extend over significant distances to determine areas suitable for attachment.[24] Therefore, the roughened surface in this study appears to show cell filopodia exploring the substrate topography for areas to which a greater surface area of the cell can adhere. Dalby et al. have observed similar morphologies of osteoblasts cultured on HAPEX, which has varying degrees of roughened topography.[13]

Itala et al.[25] analyzed silica gel and calcium phosphate formation on microroughened bioactive glass surfaces of three different compositions (13–93: 53% SiO_2, 6% Na_2O, 20% CaO, 12% K_2O, 5% MgO, 4% P_2O_5; 1–98: 55%, 4%, 22%, 9%, 5%, 4%, respectively, and 1% B2O3; 3–98: similar to 1–98). They found that formation of the silica gel layer was accelerated on the roughened surfaces, which they explain is due to the enhanced Si leaching from the surface as a result of their chemical etching procedure. However, the formation of calcium phosphate layer was equal between control and microroughened glass surfaces. They also determined that the roughened surfaces significantly enhanced the attachment of human osteoblast-like MG-63 osteosarcoma cells during the first 24 h of incubation but did not have an effect on their proliferation rate or morphology.

In our study, when cultures were supplemented with dexamethasone and beta-glycerophosphate, the formation of mineralized nodules was observed. Nodules were positively stained with alizarin red, which binds to calcium deposits. No difference in mineralization was observed between the rough and smooth surfaces. It is interesting to note, however, that no nodule formation was observed in cultures on Thermanox™ controls. It must be noted that we only studied up to 14 days and it is likely that nodules would form at later time points on the Thermanox™. Due to the presence of calcium in the Bioglass composition, this also can stain red, and therefore make observation of true mineralized nodules and areas of cells difficult. We therefore confirmed not only the presence of calcium within these nodules using Raman spectroscopy,

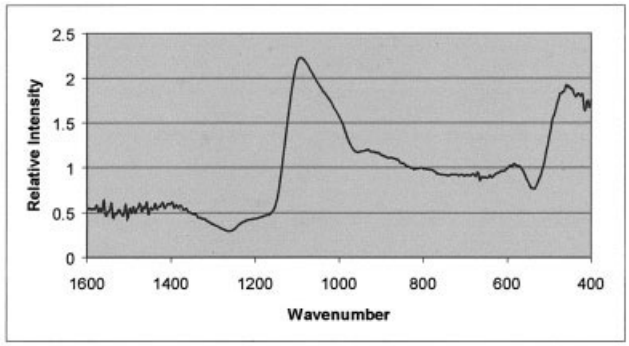

A

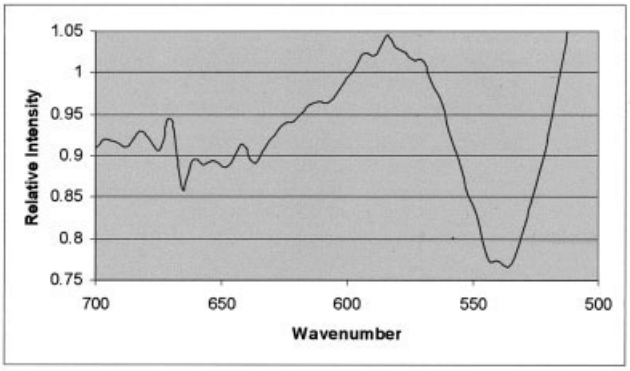

B

Figure 10. FTIR spectra (A and B) of 45S5 rough surface showing hydroxyapatite formation.

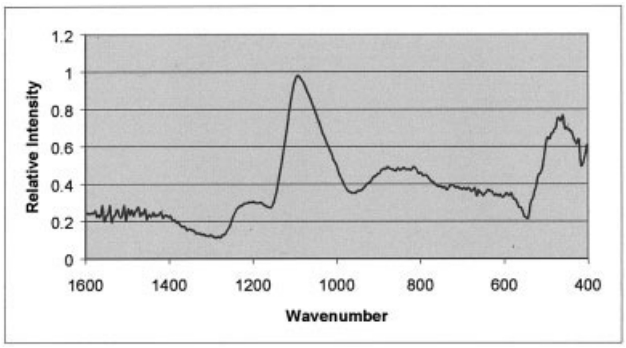

Figure 11. FTIR spectra of 45S5 smooth surface.

but also that this calcium was present in the form of hydroxyapatite.

The formation of hydroxyapatite on the smooth and rough surfaces was analyzed by FTIR to determine if there were any differences. HA formation was more rapid on the rough surface, with very little apparent on the smooth surface, showing that a rough surface was better for forming HA with these samples and conditions. The Si peak (rough) near 460 cm^{-1} is still large, indicating that the HA layer is thin or possibly discontinuous. The faster HA formation on the rough surface may have contributed to the cell morphology and nodule formation, and this is being investigated.

This study demonstrates a marked difference in morphology on roughened and smooth surfaces and that initial morphology of osteoblast spreading effects nodule formation but not mineralization of these nodules. We also demonstrate the use of Raman spectroscopy in live osteoblast cultures to analyze mineralization with greater specificity than traditional alizarin red staining. Future research will include other degrees of topography, gene expression analysis, and further investigation of mineralization by Raman spectroscopy. These results show that the roughness of the samples studied (compared to a smooth surface) improves human primary osteoblast nodule formation. Generally in the literature a highly spread cell morphology is regarded as optimum, yet in this study we show that a less spread, spiky morphology appears to lead to increased nodule formation. The roughness of sample may be beneficial *in vivo*, as it may promote more rapid bone formation at the tissue–implant interface if used for bone tissue engineering or regeneration. The bioactive glass investigated in this study was in monolithic form: however, the roughness effect observed could be translated to powder form, foamed scaffolds, or fibers to enhance the osteoblast effect *in vitro* and potentially *in vivo.*

The authors would like to thank Tim Ryder and Margaret Mobberley (Department of Histopathology, Charing Cross Hospital, London) for kind assistance with the scanning electron microscopy, Daniel Clupper, Department of Materials, Imperial College, for performing the FTIR; and Richard Chater, Department of Materials, Imperial College, for assistance with the Zygo analysis.

References

1. Hench LL, Splinter RJ, Allen WC, Greenlee TK. Bonding mechanism at the interface of ceramic prosthetic implants. J Biomed Mater Res 1971;74:1478–1570.
2. Hench LL, Wilson J. An introduction to bioceramics. Singapore: World Scientific; 1993.
3. Sepulveda P, Jones JR, Hench LL. Bioactive sol-gel foams for tissue repair. J Biomed Mater Res 2002;59:340–348.
4. Zhang K, Ma Y, Francis LF. Porous polymer/bioactive glass composites for soft-to-hard tissue interfaces. J Biomed Mater Res 2002;61:551–563.
5. Livingston T, Ducheyne P, Garino J. In vivo evaluation of a bioactive scaffold for bone tissue engineering. J Biomed Mater Res 2002;62:1–13.
6. Hench LL, West JK. Biological applications of bioactive glasses. Life Chem Rep 1996;13:187–241.
7. Oonishi H, Hench LL, Wilson J, Sugihara F, Tsuji E, Matsuura M, Kin S, Yamamoto T, Mizokawa S. Quantitative comparison of bone growth behaviour in granules of Bioglass, A-W glass ceramic and hydroxyapatite. J Biomed Mater Res 2000;51:37–46.
8. Curtis A, Wilkinson C. Topographical control of cells. Biomaterials 1997;18:1573–1583.
9. Clark P, Connolly P, Curtis ASG, Dow JAT, Wilkinson CDW. Topographical control of cell behaviour: II: Multiple grooved substrata. Development 1990;108:635–644.
10. den Braber ET, de Ruijter JE, Ginsel LA, von Recum AF, Jansen JA. Quantitative analysis of fibroblast morphology on microgrooved surfaces with various groove and ridge dimensions. Biomaterials 1996;17:2037–2044.
11. Lincks J, Boyan BD, Blanchard CR, Lohmann CH, Liu Y, Cochran DL, Dean DD, Schwartz Z. Response of MG-63 osteoblast-like cells to titanium and titanium alloy is dependent on surface roughness and composition. Biomaterials 1998;19:2219–2232.
12. Anselme K, Bigerelle M, Noel B, Dufresne E, Judas D, Iost A, Hardouin P. Qualitative and quantitative study of human osteoblast adhesion on materials with various surface roughnesses. J Biomed Mater Res 2000;49(2):155–166.
13. Dalby MJ, Di Silvio L, Gurav N, Annaz B, Kayser MV, Bonfield W. Optimizing HAPEX topography influences osteoblast response. Tissue Eng 2002;8:453–467.
14. Puppels GJ, Greve J. Whole cell studies and tissue characterisation by Raman Spectroscopy. In: Clark RJH, Hester RE, editors. Advances in spectroscopy, vol. 25. R. Chichester: John Wiley & Sons Ltd.; 1996. p 1–47.
15. Notingher I, Verrier S, Romanska H, Bishop AE, Polak JM, Hench LL. In-situ characterisation of living cells by Raman spectroscopy. Spectroscopy 2002;16;43–51.
16. Notingher I, Verrier S, Haque S, Polak JM, Hench LL. Spectroscopic study of human lung epithelial cells (A549) in culture: Living versus dead cells. Biopolymers 2003:72(4):230–240.
17. Stewart S, Shea DA, Tarnowski CB, Morris MD, Wang D, Franceschi R, Lin D-L, Keller E. Trends in early mineralisation of murine calvarial osteoblastic cultures: A Raman microscopic study, J Raman Spectrosc 2002; 33:536–543.
18. Wergedal JE, Baylink, DJ. Characterisation of cells isolated from human bone. Proceed Soc Exp Biol Med 1984;176:60–69.
19. Di-Silvio L. A novel application of two biomaterials for the delivery of growth hormone and its effects on osteoblasts. PhD Thesis 1995. Institute of Orthopaedics, University College London Medical School.

20. Sinha RK, Morris F, Sha SA, Tuan RS. Surface composition of orthopaedic implant metals regulates cell attachment, spreading and cytoskeletal organisation of primary human osteoblasts *in vitro.* Clin Orthop 1994;305:258–272.
21. Elliot JC, editor. Structure and chemistry of the apatites and other calcium orthophosphates (Studies in Inorganic chemistry series). vol. 18: New York Elsevier Science, 1994. p 169.
22. Gough JE, Scotchford CA, Downes S. Cytotoxicity of glutaraldehyde crosslinked collagen/poly (vinyl alcohol) films is by the mechanism of apoptosis. J Biomed Mater Res, 2002;61;121–130.
23. Gray C, Boyde A, Jones SJ. Topographically induced bone formation *in vitro*: Implications for bone implants and bone grafts. Bone 1996;18:115–123.
24. Hammarback JA, McCarthy JB, Palm SL, Furcht LT, Letourneau PC. Growth cone guidance by substrate bound laminin pathways is correlated to neuron-to-pathway adhesivity. Dev Biol 1988;126:29–39.
25. Itala A, Ylanen HO, Yrjans J, Heino T, Hentunen T, Hupa M, Aro HT. Characterization of microrough bioactive glass surface: Surface reactions and osteoblast responses *in vitro.* J Biomed Mater Res 2002;62:404–411.